Biointerface Research in Applied Chemistry
Open-Access Journal (ISSN: 2069-5837)

Article
Volume 13, Issue 4, 2023, 388
https://doi.org/10.33263/BRIAC134.388

Quality by Design approach for Optimization and Development of Cyclodextrin-Surfactant Complex Based Formulations for Bioavailability Enhancement of Valsartan

Lakshmanarao Potti [1,2,*], Prameela Rani Avula [3]

[1] School of Pharmacy, Jawaharlal Nehru Technological University Kakinada, Kakinada, Andhra Pradesh, India.
[2] Department of Pharmaceutics, MAM College of Pharmacy, Kesanupalli, Narsaraopet, Andhra Pradesh, India.
[3] College of Pharmaceutical Sciences, Acharya Nagarjuna University, Guntur, Andhra Pradesh, India.
* Correspondence: lakshmanp2019@gmail.com;

Received: 10.07.2022; Accepted: 11.08.2022; Published: 31.10.2022

Abstract: The main objective of the present research is to increase the oral bioavailability of Valsartan by inclusion complexes (ICVs) with a cyclodextrin-surfactant combination followed by the formulation of fast-dissolving tablets (FDTs). The solvent evaporation method was used for the preparation of ICVs. Methyl-ß-cyclodextrin and Hydroxypropyl-ß- cyclodextrin were evaluated with the combination of poloxamer 188 to get the formulations with the desired solubility. Central composite design (CCD) was used as the experimental design as a part of the quality by design (QbD) approach. The optimized ICVs were further developed into FDTs by direct compression technique. Taking concentration of povidone, type and concentration of disintegrant as the formulation factors, the FDTs were optimized using CCD. *In-vivo* bioavailability study in rats was performed for the optimized FDTs against the marketed tablets. The optimized ICVs were found to have a 3.12 mg/mL solubility. The optimized FDTs were found to be disintegrated in 18.7 sec and dissolved 90% of the dose in 6.3 min. The *In-vivo* results indicated that the FDTs exhibited rapid absorption and an increase in bioavailability by 24.1% against the marketed tablets. The results indicated that the QbD approach successfully improved Valsartan's oral bioavailability through cyclodextrin-surfactant complexation.

Keywords: bioavailability; Valsartan; cyclodextrin-surfactant complexes; fast dissolving tablets; central composite design; quality by design.

1. Introduction

Quality by design (QbD) assemblages of statistical and mathematical models. It is very useful in systemically designing dosage forms with better quality and getting desired better clinical activity. QbD will also help in finding the risks associated with dosage form development, followed by reducing the same [1]. Based on the number of dependent and independent factors, different models are available in QbD to design the products with the utmost quality. Valsartan belongs to the pharmacological class of cardiovascular drugs, which helps treat congestive heart failure, another heart disease, by controlling high blood pressure by relaxing blood vessels to allow smooth blood flow. Valsartan inhibits the aldosterone secretion from the adrenal gland and vascular smooth muscles by acting on the angiotensin II receptor [2]. Valsartan has low water solubility and dissolution-limited bioavailability, as per

the literature [3]. Some authors reported it as a biopharmaceutic classification systems (BCS) class II drug, while others reported it as a BCS class III drug [Ref: Val BCS class II or III]. Whatever the class, this drug has a low bioavailability of about 25% and needs improvement.

Cyclodextrins are sugar moieties formed with glucopyranoside rings with a lipid lipophilic cavity inside and a hydrophilic outer surface. They are differentiated as α, ß, and γ cyclodextrins based on the number of rings. Among all the available cyclodextrins, ß form is the most widely used form due to its suitable cavity size, cost-effectiveness, vast availability, and less toxicity [4]. A variety of research was performed on a number of drugs to improve their bioavailability using cyclodextrins.

To improve the bioavailability of Valsartan, different formulations include but are not limited to solid dispersions, proliposomes, mucoadhesive pellets, mesoporous silica nanoparticles, and cyclodextrin complexes. Solid dispersions are good drug delivery systems to improve limited solubility and bioavailability. Still, it is always limited by the usage of organic solvents and the requirement of special techniques like spray drying [5]. Whereas the preparation of cyclodextrin complexes is easier, the problems associated with the solid dispersions can be resolved in the case of cyclodextrin complexes. Even after many advantages, cyclodextrins also have limitations in usage due to their high amount per dose and high molecular weight. To convert the drug into the soluble cyclodextrin complex, more amount of cyclodextrin must be used, thereby leading to the increase in weight of the formulation per unit dose. To overcome this issue, only a few researchers used incorporating surfactant in the cyclodextrin complexes [6,7]. But, promising advantages of the cyclodextrin-surfactant complexes were reported in the food industry [8]. Further, surfactants can improve permeability during drug absorption by reducing interfacial tension at the biological membranes. Considering the multiple advantages of surfactants towards increasing solubility and permeability and decreasing the weight of unit dose, these cyclodextrin-surfactant complexes have great scope in exploring their application in drug delivery systems.

In the current research, inclusion complexes for Valsartan (ICVs) were prepared using poloxamer 188 as a surfactant with solvent evaporation [9]. Further, the ICVs were compressed into fast-dissolving tablets (FDTs) using suitable excipients by employing the Quality by Design approach. In the present study, central composite design (CCD) was used during the preparation of the development and optimization of cyclodextrin inclusion complexes to evaluate the concentration of cyclodextrins, Concentration of Poloxamer, type of cyclodextrins as formulation factors; and solubility as the response. CCD was also applied during the preparation of FDTs for the optimized ICVs. For the optimization of FDTs, rapid disintegration and dissolution were set as Quality target product profiles. Disintegration time and time for 90% dissolution were set as critical quality attributes. The concentration of povidone, the concentration of super-disintegrant (SD), and the Type of SD were selected as formulation factors [10]. Design analysis followed by optimization of the parameters was also performed to obtain the final formulation with rapid disintegration and faster dissolution. The final optimized FDT and valsartan-marketed tablets were subjected to *in vivo* bioavailability studies to confirm the improvement in bioavailability.

2. Materials and Methods

2.1. Materials.

Valsartan was received from Hetero Labs Pvt. Ltd, Visakhapatnam, as a gift sample, Methyl-β-CD, Hydroxypropyl-β-CD, and Poloxamer-188 were purchased from Sigma Aldrich Chemicals Co., Mumbai. Sodium starch glycolate (SSG), microcrystalline cellulose (MCC), crospovidone (CP), mannitol, and starch citrate (SC) were acquired as gift samples from BASF pharma. All other materials used belong to the analytical grade.

2.2. Preparation of cyclodextrin complexes of Valsartan (ICVs).

Cyclodextrin-surfactant complexes were developed and optimized by employing QbD; below given were the QbD parameters [11] for Valsartan Cyclodextrin inclusion complexes (ICVs):

2.2.1. Quality Target Product Profiling (QTPP).

Solubility improvement was fixed as the target or the desired outcome of the prepared ICVs to contribute to the improved dissolution there by the bioavailability of Valsartan.

2.2.2. Critical Quality Attributes (CQAs).

Critical quality attributes are typically known as the outcome of the process or the product that describes the quality of the product or process. In the current research, solubility was selected as CQA, which directly correlates with drug bioavailability.

2.2.3. Critical Process/Formulation Parameters (CPPs).

Critical process parameters are the factors that can have a possible impact on CQAs. These generally include process conditions, formulation factors, and raw material properties which can influence the quality characteristics of the final product or process. As the CPPs directly impact product quality, they need to be selected and optimized to have the products with desired quality. Based on the literature and prior experience handling other products, three formulation factors viz. The concentration of cyclodextrins, Concentration of poloxamer, and Type of cyclodextrin were selected as the CPPs.

2.2.4. Experimental Design.

The selection of a suitable experimental design will help evaluate the impact of the CPPs on the CQAs, which will directly impact the QTPP of the product. CCD was selected based on the selected QTPP, CPPs, and CQAs, and the design recommended formula compositions are shown in Table 1.

2.3. Preparation of ICVs by solvent evaporation.

Solvent removal by evaporation with the solvent combination of Dimethyl sulfoxide (DMSO) and chloroform ($CHCl_3$) at a 1:1 ratio was used to prepare ICVs. As per the suggested combinations by CCD, the specific amount of drug and cyclodextrins were dissolved in a solvent mixture containing poloxamer 188; the mixture was subjected to shaking on the orbital shaker at 100 RPM until the formation of a clear solution. Later the mixture was subjected to

drying using rotavapor at 60°C temperature and 100 mmHg pressure [12]. The dried ICVs were collected and stored until further usage.

Table 1. Combinations of the factors and their levels according to CCD for developing ICVs.

Std. order	Run order	Code	Level of Factors			Response: Solubility (mg/mL)*
			A (Conc. of CD, % w/w)	B (Conc. of Surfactant, % w/v)	C (Type of CD)	
14	1	ICV1	26.38	0.20	HP-β-CD	1.9 ± 0.3
3	2	ICV2	33.30	0.30	Methyl-β-CD	1.6 ± 0.1
8	3	ICV3	50.00	0.34	Methyl-β-CD	2.0 ± 0.2
18	4	ICV4	50.00	0.20	HP-β-CD	2.3 ± 0.4
1	5	ICV5	33.30	0.10	Methyl-β-CD	1.5 ± 0.2
11	6	ICV6	66.70	0.10	HP-β-CD	2.4 ± 0.5
5	7	ICV7	26.38	0.20	Methyl-β-CD	0.8 ± 0.2
12	8	ICV8	33.30	0.30	HP-β-CD	2.1 ± 0.3
13	9	ICV9	66.70	0.30	HP-β-CD	3.2 ± 0.5
17	10	ICV10	50.00	0.34	HP-β-CD	1.8 ± 0.4
10	11	ICV11	33.30	0.10	HP-β-CD	1.7 ± 0.1
7	12	ICV12	50.00	0.06	Methyl-β-CD	1.1 ± 0.1
9	13	ICV13	50.00	0.20	Methyl-β-CD	1.8 ± 0.3
4	14	ICV14	66.70	0.30	Methyl-β-CD	2.8 ± 0.2
15	15	ICV15	73.62	0.20	HP-β-CD	3.5 ± 0.5
6	16	ICV16	73.62	0.20	Methyl-β-CD	2.5 ± 0.3
2	17	ICV17	66.70	0.10	Methyl-β-CD	2.0 ± 0.3
16	18	ICV18	50.00	0.06	HP-β-CD	1.9 ± 0.2

2.4. Physicochemical characterization of ICVs.

2.4.1. Determination of % yield.

The % yield for the formulated ICVs was calculated by dividing the ICVs' weight by that of the total amount of raw materials used for their preparation. The yield was shown as a percentage.

2.4.2. Total drug content.

Total drug content was determined by using the shake flask method. Briefly, 10 mg equivalent ICVs were added to the 100 mL of pH 6.8 phosphate buffer and shaken for 2 hours using an orbital shaker. The media was subjected to filtration, and the collected filtrate was analyzed using spectrophotometrically with suitable dilution with pH 6.8 phosphate buffer [13].

2.4.3. Differential scanning calorimetry (DSC).

DSC was executed for the pure Valsartan and the prepared ICVs to know the nature of Valsartan after complexation. Briefly, 5 mg of the sample was dispensed and transferred into the flat aluminum pans with crimp-on lids. The sample was scanned in the range of 50°C to 400°C at 10°C speed in the presence of nitrogen at a flow rate of 20 mL/ min [14].

2.4.4. X-Ray Diffraction (X-RD).

XRD studies help in finding the nature of the API before and after complexation with cyclodextrins. In the present study, XRD was performed for pure drugs and prepared ICVs to

know their crystalline nature before and after complexation. Usually, in the XRD graphs, the sharp, highly intense peaks intimate the presence of crystallinity, whereas the blunt or irregularly shaped, less intense peaks indicate the presence of an amorphous form [15].

2.4.5. Solubility.

Solubility was determined for ICVs using an orbital shaker. Briefly, excess ICVs were placed into 10 mL of water and subjected to shaking for up to 24 hours. Later, the dispersion was filtered, and the obtained filtrate was analyzed spectrophotometrically after suitable dilution with water [16].

2.5. Design validation and optimization of ICVs.

Stat Ease Design expert software was employed to optimize the selected design; a sequential model sum of squares scrutinized the outcomes of all the there variable combinations to find the suitable statistical model for analyzing the effects of different variables on the response (solubility). The model's fitness and other factors' impact on the outcomes were evaluated using the (Analysis of variance) ANOVA test. Further optimization was performed for the input factors to get the desired solubility by the desirability functions approach [17].

2.6. Formulation of fast-dissolving tablets using the optimized ICVs.

Fast-dissolving tablets were manufactured by using the optimized ICVs with the help of rapidly dissolving excipients [18]. The tablets were manufactured by using direct compression technology [19] according to CCD by considering the concentration of binder polyvinyl pyrrolidone (PVP) in the range of 2-6% w/w (as factor A) and concentration of super disintegrant (SDis) in the range of 2-8% w/w (as factor B), and the type of super disintegrant viz. SSG, CP, and SC (as factor C) as the CPPs. The factors and their levels combinations for the development of FDTs recommended by CCD are shown in Table 2, and the manufacturing formulae per tablet are shown in Table 3.

2.7. Characterization of fast-dissolving tablets.

Weight variation, friability, and disintegration tests were performed in accordance with the Indian pharmacopeia. Packing fraction (Pf) indicates the post-compression consolidation ability of tableting powder. It can be obtained using the equation [20]

$$P_f = \frac{w}{\pi r^2 t \rho}$$

where, w, r, and t are the weight, radius, and thickness of the tablet, and ρ is the true density of the tableting powder.

A dissolution test for the FDTs of all the formulations was done as per the USP-NF specifications. Dissolution was conducted in 1000 mL of 0.067M phosphate buffer pH 6.8 with paddle apparatus maintained at 50 rpm for 30 min. Samples of 5 mL were removed and substituted with fresh medium every 5min. The samples were analyzed spectrophotometrically to obtain the % drug dissolved. The data was subjected to dissolution kinetics to determine the rate constant and time for 90% drug dissolved (T90%).

2.8. Design validation and optimization of the FDTs.

Stat-Ease Design expert software was employed to validate the sequential model sum of squares and scrutinize the selected design and the outcomes of all their variable combinations to find the suitable statistical model for analyzing the effects of the factors on the responses (DT and T90%). The model's fitness and the factors' impact on the responses were evaluated by using an ANOVA test and comparing the adjusted and predicted R^2 values. Further graphical optimization was performed for the input factors to yield the desired responses of the FDTs by the desirability functions approach [17,21].

Table 2. Combinations of the factors and their levels suggested by CCD for developing Valsartan FDTs.

S. No.	Run order	Formulation Code	Levels of the factors		
			A: Conc. of PVP (%w/w)	B: Conc. of SDis (%w/w)	C: Type of SDis.
1	18	F1	4.00	0.76	SSG
2	17	F2	2.00	2.00	SSG
3	8	F3	6.00	2.00	SSG
4	19	F4	1.17	5.00	SSG
5	15	F5	4.00	5.00	SSG
6	7	F6	6.83	5.00	SSG
7	13	F7	2.00	8.00	SSG
8	5	F8	6.00	8.00	SSG
9	2	F9	4.00	9.24	SSG
10	6	F10	4.00	0.76	CP
11	14	F11	2.00	2.00	CP
12	20	F12	6.00	2.00	CP
13	21	F13	1.17	5.00	CP
14	22	F14	4.00	5.00	CP
15	27	F15	6.83	5.00	CP
16	9	F16	2.00	8.00	CP
17	26	F17	6.00	8.00	CP
18	1	F18	4.00	9.24	CP
19	16	F19	4.00	0.76	SC
20	24	F20	2.00	2.00	SC
21	3	F21	6.00	2.00	SC
22	11	F22	1.17	5.00	SC
23	12	F23	4.00	5.00	SC
24	23	F24	6.83	5.00	SC
25	4	F25	2.00	8.00	SC
26	25	F26	6.00	8.00	SC
27	10	F27	4.00	9.24	SC

Table 3. Compositions (mg/ Unit) of Valsartan FDTs according to the CCD.

Formulation code	Name and quantity of excipients per unit dose							Unit weight (mg)
	ICVs Eq. to 40 mg Valsartan	PVP K15	Disinteg-rant	Manni-tol	Mg. stearate	Aerosil	MCC	
F1	135	12	2.28[1]	15	3	3	129.72	300
F2	135	6	6[1]	15	3	3	132	300
F3	135	18	6[1]	15	3	3	120	300
F4	135	3.51	15[1]	15	3	3	125.49	300
F5	135	12	15[1]	15	3	3	117	300
F6	135	20.49	15[1]	15	3	3	108.51	300
F7	135	6	24[1]	15	3	3	114	300
F8	135	18	24[1]	15	3	3	102	300
F9	135	12	27.72[1]	15	3	3	104.28	300
F10	135	12	2.28[2]	15	3	3	129.72	300
F11	135	6	6[2]	15	3	3	132	300
F12	135	18	6[2]	15	3	3	120	300

Formulation code	Name and quantity of excipients per unit dose							Unit weight (mg)
	ICVs Eq. to 40 mg Valsartan	PVP K15	Disinteg-rant	Manni-tol	Mg. stearate	Aerosil	MCC	
F13	135	3.51	15^2	15	3	3	125.49	300
F14	135	12	15^2	15	3	3	117	300
F15	135	20.49	15^2	15	3	3	108.51	300
F16	135	6	24^2	15	3	3	114	300
F17	135	18	24^2	15	3	3	102	300
F18	135	12	27.72^2	15	3	3	104.28	300
F19	135	12	2.28^3	15	3	3	129.72	300
F20	135	6	6^3	15	3	3	132	300
F21	135	18	6^3	15	3	3	120	300
F22	135	3.51	15^3	15	3	3	125.49	300
F23	135	12	15^3	15	3	3	117	300
F24	135	20.49	15^3	15	3	3	108.51	300
F25	135	6	24^3	15	3	3	114	300
F26	135	18	24^3	15	3	3	102	300
F27	135	12	27.72^3	15	3	3	104.28	300

2.9. In vivo bioavailability studies.

This study was carried out according to the protocol approved by the Institute Animal Ethics Committee (IAEC) of MAM College of Pharmacy, Kesanupalli, Guntur, and the approval number assigned was 1987/PO/Re/S/17/CPCSEA. Male Wistar rats aged 221 – 264g were considered for the *in vivo* bioavailability studies. The rats were maintained for a period of 7 days of 12 h cycles of light-dark in the animal house at a temperature and humidity of 22 ± 0.5 °C and 50 ± 2 RH. The rats were maintained fast overnight, allowing only water until 4 h post-dosing. The animals were grouped, consisting of 6 animals per group. Group 1 was considered as control; Group 2 was assigned to the Reference product (Valzaar 40 Tablet, Torrent Pharmaceutical Ltd.); and Group 3 was assigned to the Optimized Valsartan FDT. The animals in the Group 2 and Group 3 were administered 10 mg/kg [22] of the respective formulations. The equivalent dose weights of both formulations were separated from the respective tablets. They were checked for the drug content and ensured that they contained the desired amount of the drug. On day one of the experiment, the respective samples were administered with water orally. Samples of blood were collected from the lateral saphenous vein of the second leg at 1, 2, 3, 4, 6, 8, 12, 18, and 24 h after dosing into 2mL Eppendorf tubes containing sodium citrate as the anticoagulant. The samples were stored at -20^{o}C temperature until further procedure.

A solvent deproteinization technique [23] was adopted to extract Valsartan from the plasma samples. The plasma samples were spiked with Losartan [23] as the internal standard at 50µg/mL concentration. 200 µL of these plasma samples were added to 2 mL of Methanol and Acetonitrile at 50:50 as the deproteinization agent in a glass tube. The glass tube was vortexed for 5 min using a cyclomixer. Later, the supernatant was separated and filtered into another glass tube which was then subjected to evaporation under a nitrogen environment. Into this glass tube containing the dried residue of the drugs, 0.5 mL of the mobile was added and mixed. Then 20 µL of this solution was injected into the HPLC column for further analysis [23].

3. Results and Discussion

3.1. Physicochemical characterization of ICVs.

The prepared ICVs were evaluated for their % yield, total drug content, and solubility and also evaluated to find the physical interactions and changes in crystallinity using DSC and PXRD studies. The yields of the prepared formulation were found to be in the range of 85.7 to 97.6%, indicating a lower process loss. It was also evident that the selected preparation method and solvent system are very suitable for preparing ICVs with maximum yield. The ICVs were also evaluated for the total drug content, and the results were found to be in the range of 97.2% to 102.1%, which showed an even distribution of the drug in the cyclodextrin-surfactant complexes.

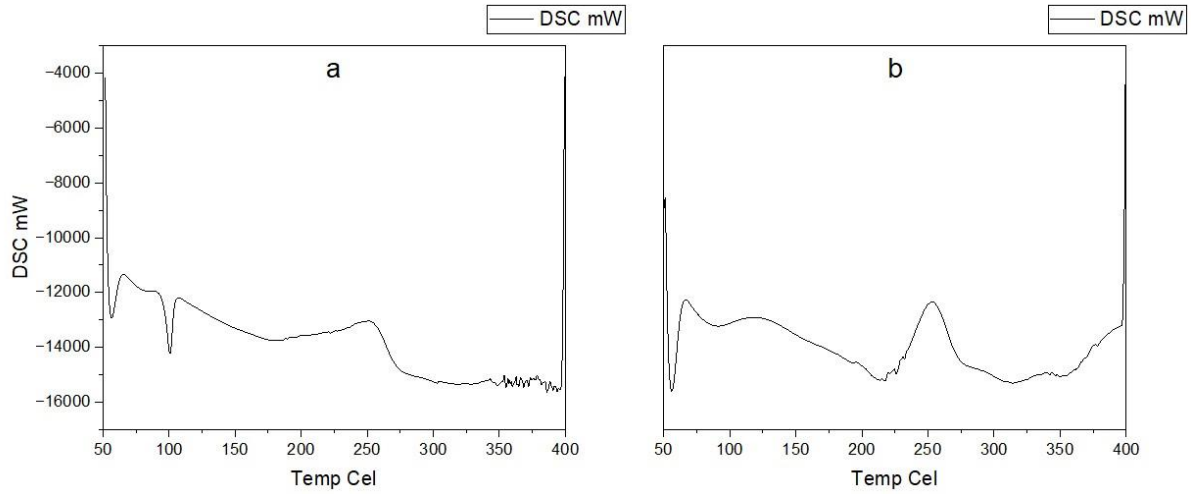

Figure 1. DSC thermograms of (**a**) Pure Valsartan and (**b**) The ICVs.

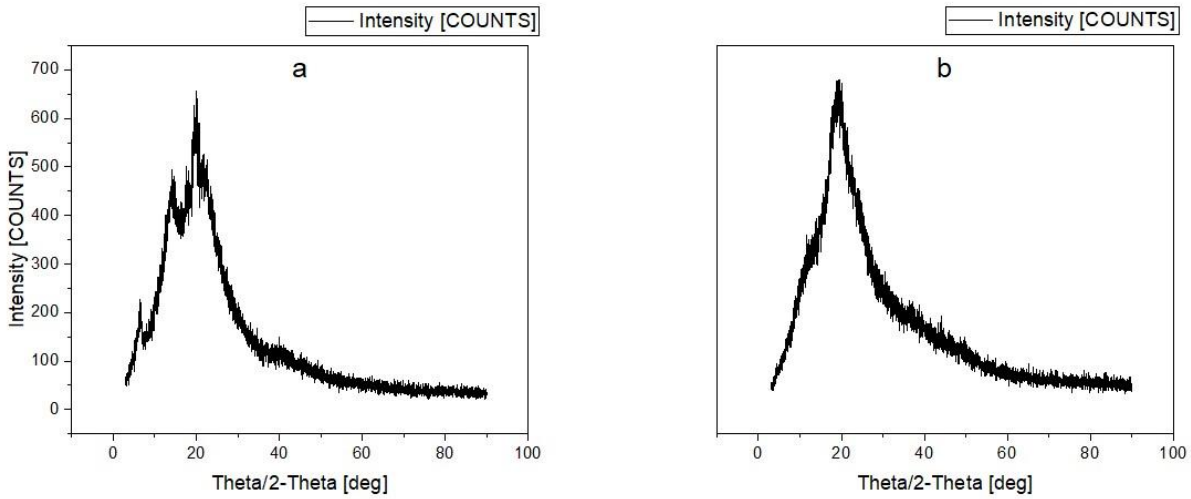

Figure 2. X-RD spectra of (**a**) Pure Valsartan and (**b**) The ICVs.

The ICVs were evaluated for any possible changes in the crystallinity of Valsartan before and after complexation. The DSC thermograms of pure valsartan and the formulated ICVs are presented in Figure 1. The thermogram of Valsartan alone had a sharp endothermic peak at 103°C [24], indicating Valsartan's crystalline nature. On the other hand, the thermogram of the ICVs did not exhibit any endothermic peak around the melting temperature of Valsartan. This might indicate the drug's conversion into an amorphous form after complexation [25].

X-ray diffraction spectra of the pure Valsartan and the ICVs were presented in Figure 2. The XRD spectrum of Valsartan was found to have more sharp, more intense peaks, but the spectrum of the ICVs was found to have broad and less intense peaks, which proved that the crystalline API was converted as an amorphous form [26]. Both the DSC and X-RD studies confirmed that the crystalline nature of Valsartan was changed into amorphous upon complexation, which might contribute towards improving solubility.

3.2. Design of experiments (DoE) analysis of the response.

The solubility results are shown in Table 1. The solubility of ICVs was found to be increased compared with the solubility of Valsartan API. The solubilities of the ICVs were obtained in the range of 0.8 to 3.5 mg/mL, which was better than the API solubility of 0.11 mg/mL. The drastic improvement in the solubility may be due to the form conversion of API into amorphous and also may be due to the highly hydrophilic nature of the cyclodextrins and the surfactant [27]. The effect of various factors on the solubility was shown using the contour plots in Figures 3(a) and 3(b)**.** The solubility was found to be high in the formulations with higher amounts of cyclodextrin, factor A, and the surfactant, factor B. This might be due to the abundant availability of more host sites in cyclodextrin for the drug, and the surfactants were able to improve the solubility by providing more interaction between the drug and cyclodextrins with the reduction in interfacial tension [28]. Along with factor A & factor B, factor C also shows its impact on solubility. ICVs formulated with methyl ß- cyclodextrin was found to have less solubility than the ICVs formulated with hydroxyl propyl ß- cyclodextrin. The more hydrophilic nature of hydroxyl propyl ß- cyclodextrin than methyl ß- cyclodextrin [29] might be a reason for this solubility enhancement. The influences of all these factors on the solubility were found to be significant by ANOVA at $p < 0.05$ and shown in Table 4.

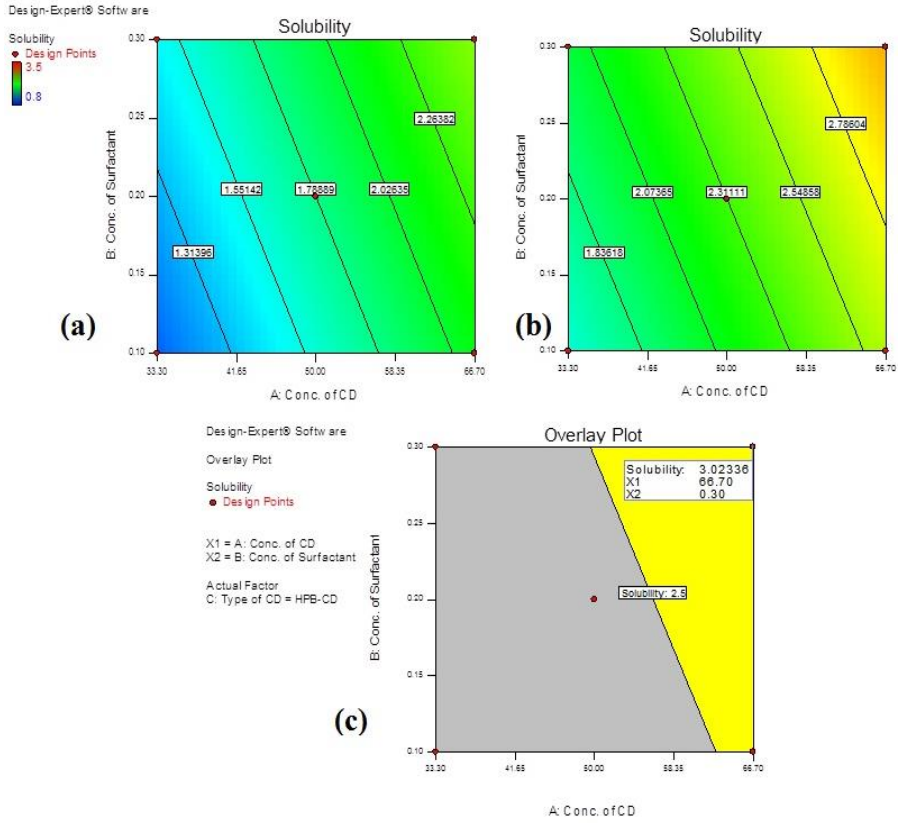

Figure 3. Contour plot showing the effect of factors A and B on the solubility of the inclusion complexes prepared with (**a**) Methyl-β-CD and (**b**) HP-β-CD; (**c**) Overlay plot indicating the design space (the yellow region) after graphical optimization.

3.3. Design validation for ICVs.

The design was validated using the sequential model sum of squares analysis followed by ANOVA to know the significance of all the factors on the response and to proceed with optimization. The results of the sequential sum of squares suggest that the linear model is a suitable one with which the effects of factors on the desired response are to be studied[30]. After the application of ANOVA, it was found that the chosen model was significant; all the selected factors were able to show an effect on the solubility that was significant at a *p*-value of <0.05, as shown in Table 4. Adjusted and predicted R^2 values were calculated and were found to be 0.7464 and 0. 6421, respectively, which were inside the difference range of 0.2. All these design validation results indicated that the applied model was suitable and could be moved to the optimization stage.

Table 4. Results of ANOVA test for response surface linear model for the solubility.

Source	SS[a]	Df[b]	MSS[c]	F value	p-Value	Inference[d]
Model	6.05	3	2.02	17.68	< 0.0001	**Significant**
A- Conc. of CD	4.17	1	4.17	36.56	< 0.0001	**Significant**
B- Conc.of Surfactant	0.65	1	0.65	5.72	0.0313	**Significant**
C-Type of CD	1.23	1	1.23	10.76	0.0055	**Significant**
Residual	1.60	14	0.11			
Cor Total	7.64	17				

Note: [a]-Sum of Squares; [b]-Degrees of Freedom; [c]-Mean Sum of Squares;
[d]-p-Value less than 0.05 indicates model terms are significant

3.4. Graphical optimization.

The desirability of the response was performed with the help of Stat-Ease Design expert software to perform the graphical optimization of the selected model [21]. The overlay plot with recommendations to get the maximum solubility of ICVs above 2.5 mg/mL is shown in Figure 3(c). The yellow part of the plot provides the combination of the variables which can provide greater than 2.5 mg/mL solubility of ICVs. The software selected 66.7% w/w of HP-ß-CD as a suitable concentration and a suitable type of cyclodextrin along with 0.3% w/v of poloxamer 188 to formulate the ICVs with the best solubility. This suggested combination was taken for another ICV preparation and analyzed for solubility. The solubility of this optimized ICV was obtained as 3.12 mg/mL, and it could correlate with the predicted value of 3.02 mg/mL. The solubility of the prepared ICVs was found to have a great increment in comparison with the solubility of pure Valsartan drug, which is 0.11 mg/mL. ICVs at this combination but without poloxamer 188 was developed, and the observed solubility was 2.37 mg/mL. This result indicated that incorporating a small amount of poloxamer could further increase the solubility without needing higher amounts of cyclodextrins. With all the above data, it was proved that the cyclodextrin-surfactant complexes could improve the drug solubility by forming a good extent of complexation with the drug and converting it into an amorphous form. Further, this optimized ICV was developed into tablets to achieve a faster disintegration rate and get 90% drug release in the lowest possible time.

3.5. Physical characterization studies of the FDTs.

The prepared FDTs were characterized for the packing fraction, porosity fraction, friability, disintegration time, and drug content, and the results are displayed in Table 5. Packing fraction and porosity fraction indicate the compressibility of the powder mixture and

strength of the compressed tablets yet having sufficient porosity to diffuse water to disintegrate the tablets. The packing fraction values of the prepared FDTs were obtained between 0.83 – 0.91; hence, the porosity fraction values were between 0.17 – 0.09. These results signified that the tablets were sufficiently hard enough yet had adequate porosity to aid disintegration [20]. Further, the friability values, which were well below the upper limit of 1%, support the physical strength of the FDTs. Drug content values were found to be in the range of 98.2 – 101.7%, thus indicating the uniform distribution of the complex form of the drug in the pre-compressed powder mixture.

Table 5. Physical characterization of the Valsartan FDTs.

Formulation	Packing fraction (P_f)	Porosity fraction ($1 - P_f$)	Friability (%)	Drug content (%)	R1: DT (sec)	R2: T90% (min.)
F1	0.86 ± 0.03	0.14 ± 0.03	0.19 ± 0.04	99.6 ± 2.3	103 ± 9	15.8 ± 1.3
F2	0.89 ± 0.04	0.11 ± 0.04	0.15 ± 0.06	98.2 ± 3.5	75 ± 6	14.1 ± 0.9
F3	0.90 ± 0.02	0.10 ± 0.02	0.36 ± 0.08	101.6 ± 1.9	89 ± 11	15.2 ± 2.1
F4	0.85 ± 0.04	0.15 ± 0.04	0.44 ± 0.03	98.7 ± 1.4	61 ± 5	12.4 ± 1.6
F5	0.87 ± 0.05	0.13 ± 0.05	0.38 ± 0.07	100.9 ± 3.2	70 ± 3	12.9 ± 1.4
F6	0.89 ± 0.03	0.11 ± 0.03	0.24 ± 0.06	99.1 ± 2.7	81 ± 4	13.8 ± 1.7
F7	0.88 ± 0.06	0.12 ± 0.06	0.17 ± 0.03	98.3 ± 2.9	48 ± 9	9.3 ± 0.8
F8	0.91 ± 0.04	0.09 ± 0.04	0.25 ± 0.04	98.6 ± 1.6	62 ± 8	11.6 ± 1.2
F9	0.84 ± 0.01	0.16 ± 0.01	0.33 ± 0.08	99.4 ± 1.3	51 ± 4	10.4 ± 1.5
F10	0.89 ± 0.03	0.11 ± 0.03	0.22 ± 0.06	100.3 ± 2.7	148 ± 13	16.5 ± 0.6
F11	0.85 ± 0.02	0.15 ± 0.02	0.19 ± 0.04	98.8 ± 2.5	127 ± 14	14.9 ± 0.8
F12	0.91 ± 0.04	0.09 ± 0.04	0.28 ± 0.03	99.7 ± 3.3	138 ± 11	15.8 ± 1.1
F13	0.84 ± 0.05	0.16 ± 0.05	0.24 ± 0.02	101.7 ± 1.6	107 ± 9	12.9 ± 0.9
F14	0.86 ± 0.02	0.14 ± 0.02	0.32 ± 0.04	100.6 ± 1.9	113 ± 14	13.7 ± 1.3
F15	0.89 ± 0.06	0.11 ± 0.06	0.16 ± 0.07	98.2 ± 2.4	121 ± 8	14.6 ± 1.8
F16	0.86 ± 0.03	0.14 ± 0.03	0.35 ± 0.03	101.4 ± 2.1	74 ± 10	8.2 ± 1.2
F17	0.85 ± 0.04	0.15 ± 0.04	0.21 ± 0.06	99.1 ± 3.6	98 ± 5	10.8 ± 0.6
F18	0.88 ± 0.07	0.12 ± 0.07	0.13 ± 0.08	99.8 ± 1.2	92 ± 6	9.6 ± 0.8
F19	0.86 ± 0.04	0.14 ± 0.04	0.13 ± 0.02	98.2 ± 2.5	109 ± 3	10.3 ± 0.5
F20	0.83 ± 0.02	0.17 ± 0.02	0.18 ± 0.04	99.7 ± 2.2	76 ± 5	9.5 ± 1.2
F21	0.89 ± 0.03	0.11 ± 0.03	0.22 ± 0.05	100.6 ± 1.8	81 ± 8	10.9 ± 0.8
F22	0.87 ± 0.05	0.13 ± 0.05	0.34 ± 0.09	101.3 ± 2.6	32 ± 2	7.7 ± 1.1
F23	0.83 ± 0.03	0.17 ± 0.03	0.26 ± 0.04	98.5 ± 3.1	40 ± 4	8.1 ± 0.5
F24	0.85 ± 0.02	0.15 ± 0.02	0.15 ± 0.04	99.2 ± 1.4	49 ± 3	8.5 ± 0.7
F25	0.88 ± 0.06	0.12 ± 0.06	0.27 ± 0.06	102.1 ± 2.6	24 ± 6	6.1 ± 0.3
F26	0.91 ± 0.04	0.09 ± 0.04	0.38 ± 0.05	98.9 ± 1.8	40 ± 5	7.2 ± 0.4
F27	0.86 ± 0.03	0.14 ± 0.03	0.32 ± 0.07	99.4 ± 2.9	27 ± 3	5.9 ± 0.5

3.6. DoE analysis of the responses.

Disintegration time (DT) was taken as Response 1(R1), and the results for all the FDTs are shown in Table 5. The sequential sum of squares analysis was performed with the Design Expert software to understand the nature of the influence of the factors on the DT. This analysis indicated that the factors had a quadratic effect on the DT. The factors' influences on the DT are shown in Figures 4(a) and 4(b). Higher concentrations of PVP (factor A) resulted in increased disintegration time. This might be because the PVP's enhanced binding capacity at higher levels could prolong the disintegration process. Another common finding with the concentration of super disintegrant (factor B) was observed as an increase in its level decreased the DT. More disintegrant particles at higher concentrations would absorb more water and swell to a greater extent which might break the tablet rapidly. An interesting observation with the factor C was observed that SC caused the fastest disintegration among the three and was

followed by SSG and CP in the order. This could be attributed to the greatest swelling index of SC, which was around 1400 [31] against around 300 for SSG [32] and much lesser for CP [33]. Even though CP had a specific greater surface among the three, the swelling index was the principal determining factor here.

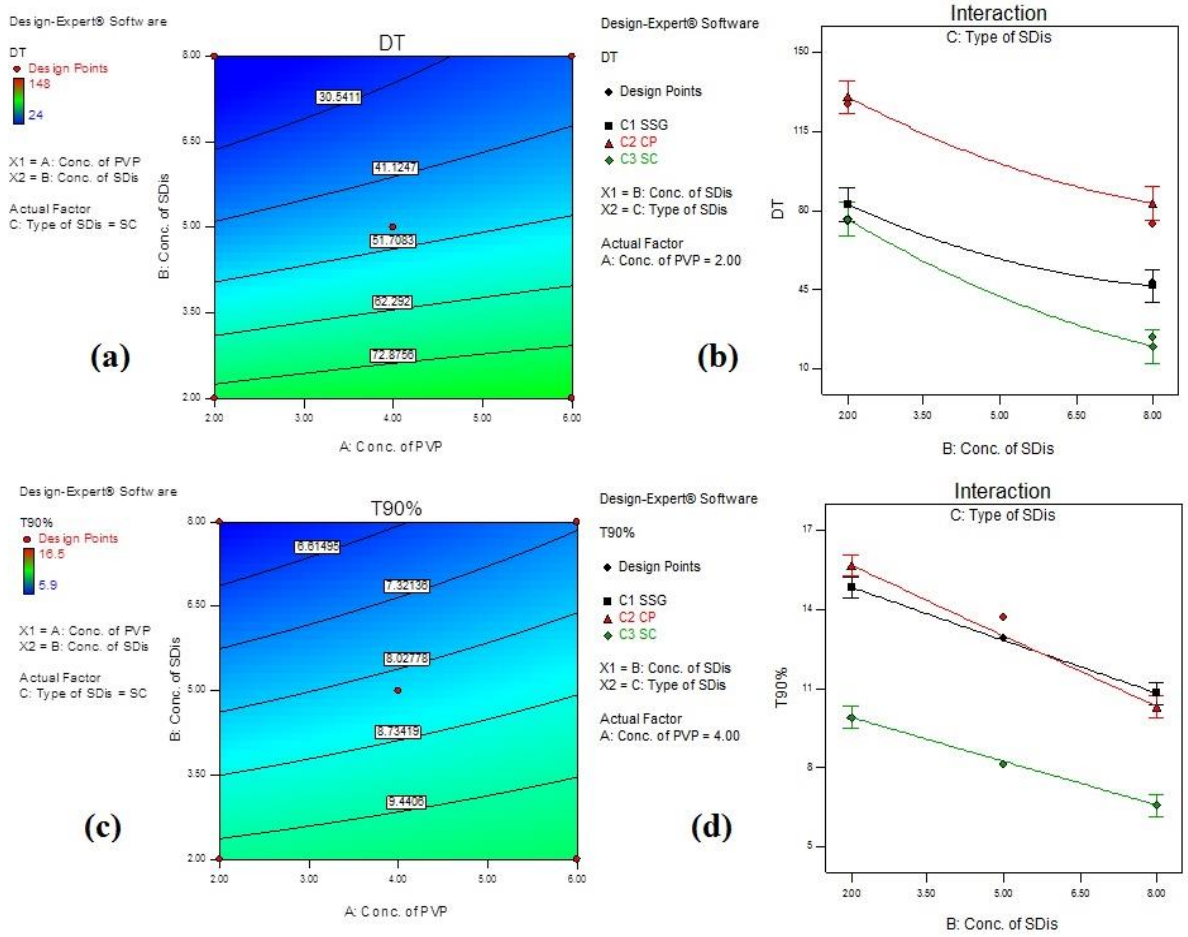

Figure 4. (**a**) Contour plot showing the effect of the factors A and B on DT; (**b**) Interaction plot showing the effect of Factor C on DT; (**c**) Contour plot showing the effect of the factors A and B on T90%; and (**d**) Interaction plot showing the effect of Factor C on T90%.

The data obtained from the dissolution test was fitted into zero-order and first-order kinetics, and it was found that these follow first-order kinetics. Using the first-order kinetics, the time necessary for the dissolution of 90% of the drug dose (T90%) was calculated from the dissolution rate constants, and the data is shown in Table 5. The sequential sum of squares analysis for this Response (R2) indicated that the factors had two factorial interaction (2FI) effects on the T90%, and the influences were shown in Figures 4(c) and 4(d). An increase in the PVP concentration (factor A) resulted in increased T90% values. This could be attributed to the decreased dissolution rate because the increased binding capacity at higher PVP levels needed more time to dissolve 90% of the drug. These results were in correlation with the DT results. The superdisintegrants concentration (factor B) had a negative effect: an increase in its level resulted in decreased T90% values. This effect is obvious that higher amounts of disintegrants make the tablets disintegrate readily, which further aid dissolution, and hence the T90% values were decreased [34]. FDTs prepared with SC exhibited rapid dissolution and minimum T90% values compared to SSG and CP. The order of influence of the disintegrants could be due to their swelling behavior, which was the highest for SC, followed by SSG and CP [31-33]. The rapid and highest degree of swelling made the FDTs break readily and the

particles available with a more hydrophilic environment. These effects of the superdisintegrants on T90% were correlated with those on the DT.

Table 6. Results of ANOVA test for response surface quadratic model for the DT (R1).

Source	SS[a]	Df[b]	MSS[c]	F value	p-Value	Inference[d]
Model	29932.11	11	2721.10	50.98	< 0.0001	**Significant**
A-Conc. of PVP	1015.62	1	1015.62	19.03	0.0006	**Significant**
B-Conc. of SDis.	10782.34	1	10782.34	202.03	< 0.0001	**Significant**
C-Type of SDis.	17064.00	2	8532.00	159.86	< 0.0001	**Significant**
AB	48.00	1	48.00	0.90	0.3580	
AC	9.33	2	4.66	0.087	0.9168	
BC	415.69	2	207.84	3.89	0.0434	**Significant**
A^2	3.19	1	3.19	0.060	0.8103	
B^2	312.00	1	312.00	5.85	0.0288	**Significant**
Residual	800.56	15	53.37			
Cor Total	30732.67	26				

Note: [a]-Sum of Squares; [b]-Degrees of Freedom; [c]-Mean Sum of Squares; [d]-p-Value less than 0.05 designates model terms are significant.

Table 7. Results of ANOVA test for response surface 2-factorial interaction model for the T90% (R2).

Source	SS[a]	Df[b]	MSS[c]	F value	p-Value	Inference[d]
Model	253.18	9	28.13	85.31	< 0.0001	**Significant**
A-Conc. of PVP	9.27	1	9.27	28.11	< 0.0001	**Significant**
B-Conc. of SDis.	107.60	1	107.60	326.31	< 0.0001	**Significant**
C-Type of SDis.	131.10	2	65.55	198.79	< 0.0001	**Significant**
AB	0.56	1	0.56	1.71	0.2086	
AC	0.35	2	0.18	0.54	0.5942	
BC	4.29	2	2.14	6.50	0.0080	**Significant**
Residual	5.61	17	0.33			
Cor Total	258.79	26				

Note: [a]-Sum of Squares; [b]-Degrees of Freedom; [c]-Mean Sum of Squares; [d]-p-Value less than 0.05 designatesmodel terms are significant.

3.7. Design validation for FDTs.

The selected CCD, along with the quadratic model for the DT (R1) and two-factorial interaction model for the T90% (R2) were subjected to the ANOVA, and the results were shown in Tables 6 and 7. These results indicated that the selected models, the influences of all three factors, and the responses were significant at $p < 0.05$. The adjusted and predicted R^2 values for the R1 were 0.9548 and 0.9157, respectively, and for the R2 were 0.9669 and 0.9403, respectively. The adjusted R^2 value has differed from the predicted R^2 well below 0.2 in the case of both responses, which further confirmed that the selected experimental design and the models were significant enough to proceed for further optimization.

3.8. Graphical optimization.

The desirability functions approach was adopted to perform the graphical optimization. The desirability constraints were set as within the range for all the factors. The desirability constraints for the responses were set in accordance with the desired quality of the FDTs, which should have rapid disintegration and dissolution. So that constraint for the R1 was set as a minimum with an upper limit of 30 sec. and for the R2 was set as a minimum with an upper limit of 8 min. At these set constraints, the results of the graphical optimization given by the software as an overlay plot are shown in Figure 5. The yellow color region of the plot, known

as the design space, indicates any combination of the factors in this space provides the FDTs with maximum desirable response values. The software identified one such best combination, and the predicted values of the responses at this combination are shown in the overlay plot in Figure 5. A new formulation of FDTs by taking this combination of the factors was prepared and subjected to disintegration and dissolution tests to obtain the DT and T90% values. The obtained experimental values of DT and T90% were 18.7 sec. and 6.3 min. These values were found inside the 95% confidence interval range of the predicted values. This result indicated that the optimization was successful, and this formulation of the FDTs was considered the optimized formulation with rapid disintegration and dissolution.

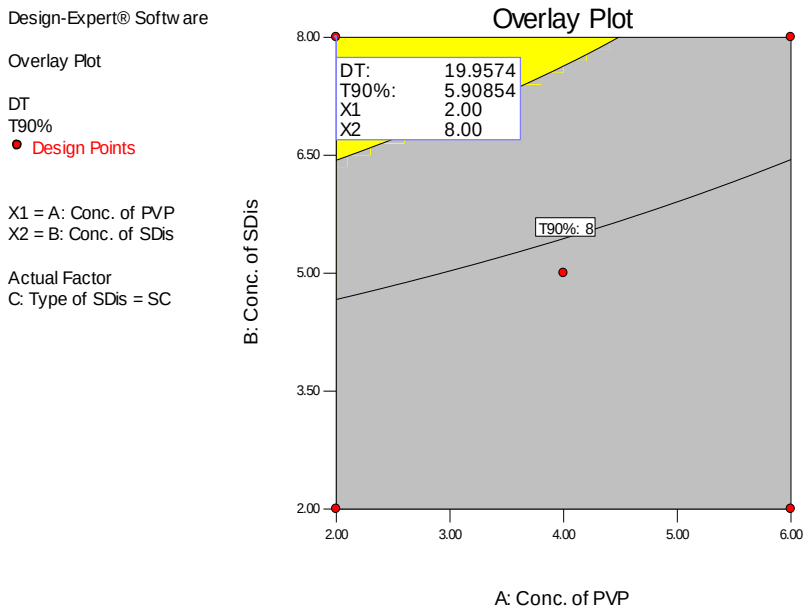

Figure 5. Overlay plot showing the design space for the set desirability criteria.

3.9. In vivo bioavailability studies.

The *in vitro* efficiency of the optimized Valsartan FDTs had to be justified by the *in vivo* studies. For this purpose, *in vivo* bioavailability studies were performed to compare further its effectiveness in relation to the marketed tablet, Valzaar 40. The time versus plasma drug concentration profiles for both formulations is shown in Figure 6. This data was subjected to non-compartmental analysis using PK solver software. The results of the pharmacokinetic parameters from the non-compartmental analysis are shown in Table 8. Comparing the maximum plasma drug concentration (C_{max}) and time for C_{max} (T_{max}) of the FDTs and the marketed tablets, the lesser T_{max} and higher C_{max} of the FDTs indicated that the rate and extent of the absorption of Valsartan from the FDTs were higher than from the marketed tablets [35]. This could be due to the high solubility of Valsartan from the FDTs due to its complex form with the cyclodextrin and the surfactant; also, the rapid disintegration of the FDTs due to the incorporation of superdisintegrant. Further, the surfactant poloxamer 188 in the complex form of the drug might also contribute to the increased absorption of Valsartan. Because the surfactants reduce the interfacial tension between the gastrointestinal (GI) fluids and the GI membrane, which can increase the diffusivity of the drug, the bioavailability can be increased. The increased bioavailability of the FDTs was also supported by the area under the curve (AUC) values which were 960.8 and 774.3µg.h/mL, respectively, for the FDTs and the marketed tablets. The differences in all three bioavailability indicating parameters between the two formulations were found to be statistically significant at $p < 0.05$ by ANOVA test. A 24.1%

increase in the bioavailability in terms of AUC for the FDTs indicated that the objective of enhancing bioavailability of Valsartan was successfully achieved.

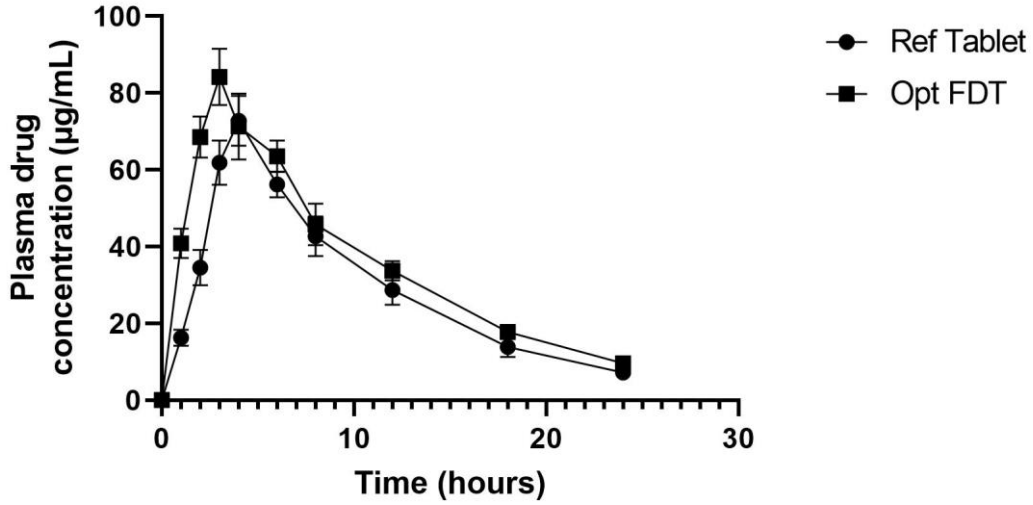

Figure 6. Valsartan plasma concentration-time profiles of the optimized FDT and the marketed tablets.

Table 8. Pharmacokinetic parameters of Valsartan from the optimized FDTs and the marketed tablets.

S. No.	Pharmacokinetic property	Result[#]	
		Reference Tablet	Optimized FDT
1	C_{max} (µg/mL)*	72.8 ± 4.1	84.2 ± 5.4
2	T_{max} (h)*	3.67 ± 0.6	2.67 ± 0.6
3	AUC_{0-t} (µg.h/mL)	710.9 ± 48.5	869.1 ± 61.2
4	$AUC_{0-\infty}$ (µg.h/mL)*	774.3 ± 52.2	960.8 ± 72.5
5	$t_{1/2}$ (h)	6.1 ± 0.4	6.6 ± 0.5
6	k_e (h^{-1})	0.114 ± 0.007	0.105 ± 0.008
7	V_d (L/kg)	0.11 ± 0.01	0.10 ± 0.02
8	Cl_T (L/h)	0.013 ± 0.0003	0.01 ± 0.001

[#] the results are expressed as Average ± Standard deviation
* the difference between the values from the Reference Tablet and the Optimized FDT was statistically significant at $p < 0.05$
$t_{1/2}$: Elimination half-life; k_e: Elimination rate constant; V_d: Apparent volume of distribution; Cl_T: Total body clearance

4. Conclusions

The ICVs-based fast-dissolving tablets were formulated to improve the bioavailability of Valsartan using Qbd as a tool using Stat-Ease software to get the finished product with desired quality. The ICVs were formulated using the experiments suggested by the CCD design, and the design was analyzed for its significance using the sum of squares analysis followed by the ANOVA. The formula was optimized to improve solubility; the optimized formula suggested by the software contains the HP-ß- CD as a type of cyclodextrin at a concentration of 66.70% w/w with a surfactant concentration of 0.30% w/w. The improved solubility of Valsartan was 3.12 mg/mL after formulating the optimized ICVs. Later the ICVs were formulated as FDTs using another CCD design with an objective of FDTs with lower disintegration time and lesser T90%. The DoE analysis confirmed that the selected design and the statistical model were significant, as all the factors significantly influenced the responses. Further graphical optimization revealed the optimized formulation of the FDTs that comprises 2% w/w PVP as a binder and 8% w/w of Starch citrate as super disintegrants. The suggested combination was formulated and analyzed for the disintegration time and T90%. The

disintegration time and the T90% of the optimized FDT were found to be 18.7 sec. and 6.31 min. respectively indicating rapid disintegration and dissolution. Finally, the *in vivo* bioavailability studies confirmed the improved solubility of the Valsartan and its rapid dissolution rate from the FDTs by showing a 24.1% higher bioavailability compared to the marketed tablets. These results designated the improvement of solubility and dissolution rate. Hence, the bioavailability of Valsartan was effectively achieved through the development of ICVs followed by FDTs using the QbD approach.

Funding

The authors did not receive any external funding to carry out this research.

Acknowledgments

The authors acknowledge the management of MAM College of Pharmacy, Kesanupalli, and the authority of JNT University Kakinada for providing the necessary support to execute this research work.

Conflicts of Interest

The authors declare that there are no conflicts of interest.

References

1. Srikar, G.; Rani, A.P. Study on influence of polymer and surfactant on *in vitro* performance of biodegradable aqueous-core nanocapsules of tenofovir disoproxil fumarate by response surface methodology. *Brazilian. J. Pharm. Sci*. **2019**, *55*, e18736, http://dx.doi.org/10.1590/s2175-97902019000118736.
2. Sindhi, C.R.; Chaudhari, P.M.; Akarte, A.M.; Wagh, K.S.; Pati, P.H. Develop and evaluate novel drug delivery system of valsartan for treatment of hypertension: A review. *GSC Biol. Pharm. Sci*. **2021**, *15*, 302-306, https://doi.org/10.30574/gscbps.2021.15.3.0179.
3. Prieto, C.; Evtoski, Z.; Pardo-Figuerez, M.; Hrakovsky, J.; Lagaron, J.M. Nanostructured valsartan microparticles with enhanced bioavailability produced by high-throughput electrohydrodynamic room-temperature atomization. *Mol. Pharm.* **2021**, *18*, 2947-2958, https://doi.org/10.1021/acs.molpharmaceut.1c00098.
4. Morin-Crini, N.; Fourmentin, S.; Fenyvesi, É.; Lichtfouse, E.; Torri, G.; Fourmentin, M.; Crini, G. 130 years of cyclodextrin discovery for health, food, agriculture, and the industry: A review. *Environ. Chem. Lett.* **2021**, *19*, 2581-2617, https://doi.org/10.1007/s10311-020-01156-w.
5. Dhande, L.B.; Deshmukh, M.T.; Khopade, A.N.; Shete, R.V.; Kunjir, V.V. A review on solubility enhancement by solid dispersion method. *J. Drug. Deliv. Ther*. **2021**, *11*, 182-187, http://dx.doi.org/10.22270/jddt.v11i1.4489.
6. Arora, P.; Singh, J.; Chadha, R.E. Physicochemical characterization and evaluation of telmisartan: hydroxypropyl-βcyclodextrin: Tween 80 inclusion complex. *Int. J. Pharm. Pharm. Sci.* **2017**, *9*, 51-58, https://doi.org/10.22159/ijpps.2017v9i9.19058.
7. Araujo, L.D.; Lazzara, G.; Chiappisi, L. Cyclodextrin/surfactant inclusion complexes: An integrated view of their thermodynamic and structural properties. *Adv. Colloid. Interface. Sci*. **2021,** *289*, 102375, https://doi.org/10.1016/j.cis.2021.102375.
8. Valente, A.J.; Soderman, O. The formation of host–guest complexes between surfactants and cyclodextrins. *Adv. Colloid. Interface. Sci*. **2014**, *205*, 156-176, https://doi.org/10.1016/j.cis.2013.08.001.
9. Goh, S.Q.; Adnan, R.; Rahim, N.Y. Mini review on synthesis and characterization methods for ternary inclusion complexes of cyclodextrins with drugs. *Malays. J. Chem*. **2022**, *24*, 54-72, https://doi.org/10.55373/mjchem.v24i1.1266.

10. Nerella, A.; Nagabhushanam, M.V. Orodispersible films of meloxicam inclusion complexes for bioavailability enhancement: Optimization and development through quality by design approach. *Int. J. Pharm. Investig*. **2021**, *11*, 420-425, https://www.jpionline.org/index.php/ijpi/article/view/1218.
11. Kengar, M.D.; Tamboli, J.A.; Magdum, C.S. Quality by design- A review. *PharmaTutor*. **2019**, *7*, 48-51, http://dx.doi.org/10.29161/PT.v7.i4.2019.48.
12. Rosaini, H.; Sandra, N.; Asra, R.; Halim, A. Characterization of celecoxib β-cyclodextrin inclusion complexes using solvent evaporation method. *Asian j. Pharm. Res. Dev*. **2021**, *9*, 41-47, http://dx.doi.org/10.22270/ajprd.v9i61037.
13. Garg, A.; Singh, S. Targeting of eugenol-loaded solid lipid nanoparticles to the epidermal layer of human skin. *Nanomedicine*. **2014**, *9*, 1223-1238, https://doi.org/10.2217/nnm.13.33.
14. Singadi, R.; Gharge, S.; Pote, S.; Suryawanshi, S.S.; Maste, M.M.; Koli, R. Application of differential scanning calorimetry to study the interpretation on herbal medicinal drugs: A review. *TMR Pharmacol Res*. **2022**, *2*, 6, https://doi.org/10.53388/PR202202006.
15. Ali, A.; Chiang, Y.W.; Santos, R.M. X-ray diffraction techniques for mineral characterization: A review for engineers of the fundamentals, applications, and research directions. *Minerals*. **2022**, *12*, 205, https://doi.org/10.3390/min12020205.
16. Alopaeus, J.F.; Gobel, A.; Breitkreutz, J.; Sande, S.A.; Tho, I. Investigation of hydroxypropyl-β-cyclodextrin inclusion complexation of two poorly soluble model drugs and their taste-sensation-Effect of electrolytes, freeze-drying and incorporation into oral film formulations. *J. Drug Deliv. Sci. Technol*. **2021**, *61*, 102245, https://doi.org/10.1016/j.jddst.2020.102245.
17. Chakraborty, P.; Dey, S.; Parcha, V.; Bhattacharya, S.S.; Ghosh, A. Design expert supported mathematical optimization and predictability study of buccoadhesive pharmaceutical wafers of loratadine. *BioMed Res. Int.* **2013**, *2013*, 197398, http://dx.doi.org/10.1155/2013/197398.
18. Olayemi, O.J.; Nock-Anyebe, S. Evaluation of Novel co-processed excipient for fast disintegration of aspirin tablet formulations. *J. Pharm. Bioresources*. **2021**, *18*, 1-11, https://dx.doi.org/10.4314/jpb.v18i1.1.
19. Shwetha-Margret, J.L.; Madhavi, BLR. Study of direct compression method for the preparation of quinapril hydrochloride tablets. *Asian. J. Pharm. Clin. Res*. **2020**, *13*, 202-11, https://doi.org/10.22159/ajpcr.2020.v13i1.34005.
20. Gupta, B.; Kumar, S. Fast dissolving tablets of fexofenadine hydrochloride by melt technology: Formulation and characterization. *Int. J. Pharm. Sci. Res*. **2018**, *9*, 1226-1230, https://doi.org/10.13040/ijpsr.0975-8232.9(3).1226-30.
21. Srikar, G.; Rani, A.P. Tenofovir loaded poly (lactide-co-glycolide) nanocapsules: Formulation optimization by desirability functions approach. *Indian J. Pharm. Edu. Res*. **2020**, *54*, S230-S240, https://doi.org/10.5530/ijper.54.2s.79.
22. Liu, Y.; Zhang, J.; Wu, D.; Cui, L. Pharmacokinetic interaction study between ligustrazine and valsartan in rats and its potential mechanism. *Pharm. Biol*. **2020**, *58*, 1299-1302, https://doi.org/10.1080/13880209.2020.1859554.
23. Reddy, M.S.; Kumar, L.; Attari, Z.; Verma, R. Statistical optimization of extraction process for the quantification of valsartan in rabbit plasma by a HPLC method. *Indian J. Pharm. Sci*. **2017**, *79*, 16-28, https://doi.org/10.4172/pharmaceutical-sciences.1000196.
24. Skotnicki, M.; Gaweł, A.; Cebe, P.; Pyda, M. Thermal behavior and phase identification of valsartan by standard and temperature-modulated differential scanning calorimetry. *Drug Dev. Ind. Pharm*. **2013**, *39*, 1508-1514, https://doi.org/10.3109/03639045.2012.704379.
25. Syed, I.A.; Patro, C.; Alshanberi, A.M.; Ansari, S.A. Statistical designing and characterization of valsartan oral disintegrating tablet. *Adv. Pharmacol. Pharm.* **2021**, *9*, 33–44, https://doi.org/10.13189/app.2021.090301.
26. Kumar, A.; Ramisetty, K.A.; Bordignon, S.; Hodnett, B.K.; Davern, P.; Hudson, S. Preparation, stabilisation, isolation and tableting of valsartan nanoparticles using a semi-continuous carrier particle mediated process. *Int. J. Pharm*. **2021**, *597*, 120199, https://doi.org/10.1016/j.ijpharm.2021.120199.
27. Nousheen, L.; Rajasekaran, S.; Qureshi, M.S. Solubility enhancement of lornoxicam with poloxamer 188 by solvent evaporation method. *Int. J. Health Sci*. **2022**, *6*, 8186–8195, https://doi.org/10.53730/ijhs.v6nS1.6847.
28. Mbah, C.J.; Ozuo, C.O. Effect of surfactants on the solubility and intrinsic dissolution rate of sparfloxacin. *Pharmazie*. **2011,** *66*, 192-194, https://doi.org/10.1691/ph.2011.0264.

29. Maheriya, P.M. Cyclodextrin: a promising candidate in enhancing oral bioavailability of poorly water soluble drugs. *MOJ Bioequiv. Availab.* **2017**, *3*, 60-63, https://doi.org/10.15406/mojbb.2017.03.00034.
30. Kousha, M.; Tavakoli, S.; Daneshvar, E.; Vazirzadeh, A.; Bhatnagar, A. Central composite design optimization of Acid Blue 25 dye biosorption using shrimp shell biomass. *J. Mol. Liq*. **2015**, *207*, 266-273, http://dx.doi.org/10.1016/j.molliq.2015.03.046.
31. Debnath, S.; Gayathri, V.G.; Swetha D.; Babu, M.N. Evaluation of disintegration efficacy of starch citrate in tablet formulations. *Asian J. Pharm. Res*. **2020**, *10*, 73-80, http://dx.doi.org/10.5958/2231-5691.2020.00014.3.
32. Edge, S.; Miller, R.W. Sodium starch glycolate. In *Handbook of Pharmaceutical Excipients*, 5th ed.: Row, R.C., Sheskey, P.J., Owen, S.C., Eds.: Pharmaceutical Press, London, UK, 2005: pp. 701-704.
33. Zhao, N.; Augsburger, L.L. The influence of swelling capacity of superdisintegrants in different pH media on the dissolution of hydrochlorothiazide from directly compressed tablets. *AAPS Pharmscitech*. **2005**, *6*, E120-126, https://doi.org/10.1208/pt060119.
34. Mahours, G.M.; Shaaban, D.E.; Shazly, G.A.; Auda, S.H. The effect of binder concentration and dry mixing time on granules, tablet characteristics and content uniformity of low dose drug in high shear wet granulation. *J. Drug Deliv. Sci. Technol*. **2017**, *39*, 192-199, https://doi.org/10.1016/j.jddst.2017.03.014.
35. van den Broek, A.K.; Prins, J.M.; Visser, C.E.; van Hest, R.M. Systematic review: The bioavailability of orally administered antibiotics during the initial phase of a systemic infection in non-ICU patients. *BMC Infect. Dis*. **2021**, 21, 285, https://doi.org/10.1186/s12879-021-05919-w.